THE EUROPEAN
PHYSICAL JOURNAL PLUS

Extended range Bonner sphere spectrometer for high-elevation neutron measurements

A. Fontanilla[1,a]**, A. Calamida**[1]**, A. I. Castro Campoy**[1]**, C. Cantone**[1]**, A. Pietropaolo**[1,2,b] (ID)**, J. M. Gomez-Ros**[1,3]**,**
V. E. MontiMafucci[4,5]**, S. Vernetto**[4,5]**, A. Pola**[6]**, D. Bortot**[6]**, R. Bedogni**[1]

[1] INFN, Laboratori Nazionali di Frascati, via Enrico Fermi 40, 00044 Frascati, Italy
[2] ENEA Dept. Fusion and Technologies for Nuclear Safety and Security, Frascati, Italy
[3] CIEMAT, Av. Complutense 40 - 28040, Madrid, Spain
[4] Università degli Studi di Torino, via P. Giuria 1, 10125 Turin, Italy
[5] INFN, Sezione di Torino, via P. Giuria 1, 10125 Turin, Italy
[6] Dipartimento di Energia, Politecnico di Milano, via La Masa 34, 20156 Milan, Italy

Abstract A Bonner sphere spectrometer was designed for the measurement of cosmic neutrons at high elevation within the INFN-based project SAMADHA. The spectrometer consists of 8 moderating spheres (6 polyethylene and 2 polyethylene plus high atomic number inserts), each embedding a cylindrical ^{3}He proportional counter. The response matrix was calculated with MCNP6. In view of the very low counting rates expected in the environment, specific design criteria were adopted to prevent non-neutron signals. The spectrometer was exposed in a reference ^{241}Am–Be neutron field at *Politecnico di Milano*, which allowed the estimation of the overall uncertainty of the simulated response matrix of about $\pm 2\%$.

1 Introduction

The geomagnetic field acts as one of Earth's barriers against cosmic radiations. At high altitudes, the radiation environment in the Earth's atmosphere is composed of galactic cosmic rays and solar particles. When this primary radiation interacts with the atmosphere, cascades of secondary radiation consisting of charged particles, muons, gamma rays, mesons, and neutrons are produced in turn reaching the ground. The penetrating capability of cosmic radiation to the Earth's magnetic field depends on its magnetic rigidity. Below the geomagnetic rigidity cut-off, incident radiations will be deflected back to space. In a large region of Brazil and South America, the geomagnetic field has the lowest intensity ($|\vec{B}| < 32,000$ nT) around the world, approximately 30% lower than areas with the same altitude and latitude [1, 2]. This is called the South Atlantic Anomaly (SAA) and is progressively expanding and drifting westward and southward [1, 3–5]. Compared to other areas with similar altitude and latitude, the SAA experiences more intense fields of secondary radiations at ground level. Due to high radiation weighting factor [6], the neutron component is relevant for the radiation protection of the public. The SAMADHA (South Atlantic Magnetic Anomaly Dosimetry at High Altitude) project aims to investigate the neutron fields in the SAA, expecting to provide new data in favour of the radiation protection, space weather, and atmosphere science fields. Key instrument for such studies will be the extended Bonner sphere spectrometer developed at INFN-Frascati and described in this work.

2 Experimental set-up

The SAMADHA extended range Bonner sphere spectrometer (ERBSS) (Fig. 1) was designed with the idea of establishing a trade-off between sensibility, spectrometric capability in the desired energy range, cost for building and shipping, portability, and availability of existing low-cost electronics. The system is composed of the following:

- *Eight moderating spheres*. To take advantage of existing electronics readout, the number of spheres was fixed to eight, two of them with extended energy range. The polyethylene spheres have diameter 80, 100, 120, 150, 170, and 200 mm, whilst the extended range spheres feature diameter 200 mm and include lead or iron inserts, promoting the detection of neutrons above 20 MeV through (n,xn) reactions (Fig. 2). Because the system will be shipped to remote locations at high elevation, its weight should be

a e-mail: Aixeen.Fontanilla@lnf.infn.it

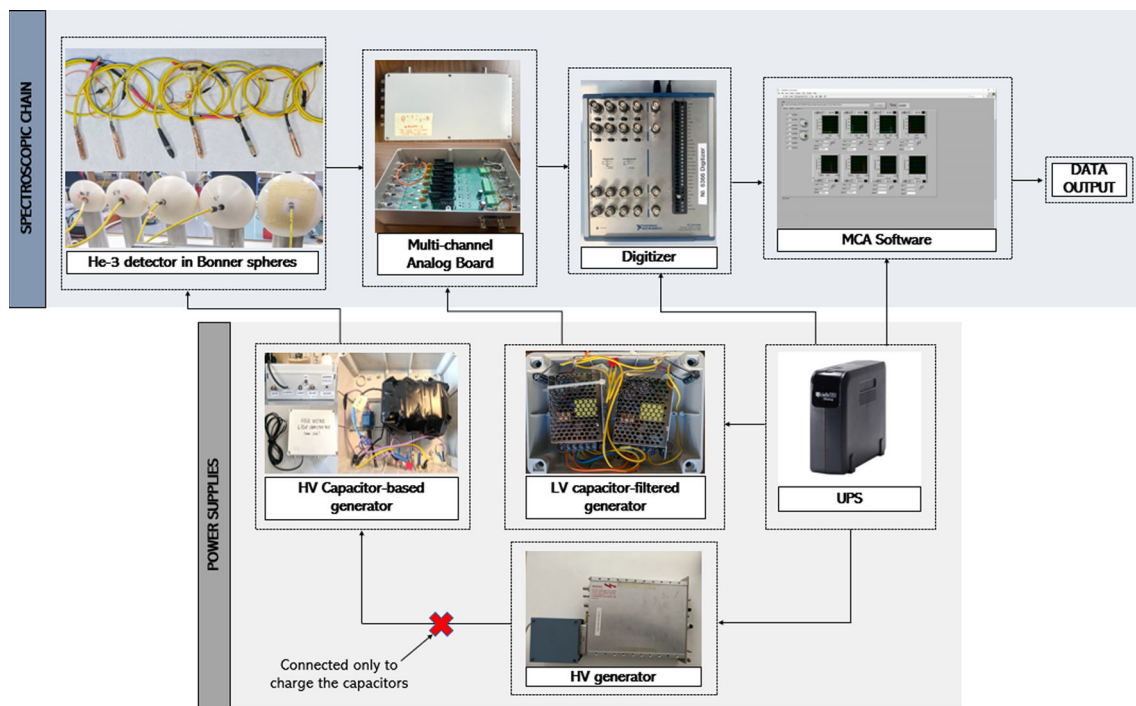b e-mail: antonino.pietropaolo@enea.it (corresponding author)

Fig. 1 SAMADHA extended range Bonner sphere spectrometer

as low as possible to minimize shipping costs. Thus, the lead or iron inserts are in the form of metal bullets (1.5 mm in diameter) that can be procured easily at very low-cost worldwide. As a term of comparison, an identical 200 mm sphere with a solid lead insert was also fabricated. The spectrometric capability of such a set of spheres is demonstrated in Sect. 3.

- *Cylindrical ^{3}He (VacuTec type 70 060) proportional counters* (also described in Ref. [7]). These ^{3}He detectors have effective volume $V_{eff} = 2.8$ cm^3, and effective length $L_{eff} = 40$ mm. The filling gas pressure is 10 bar. Their steel capsule has external diameter 1.27 cm and total length 5.4 cm. To minimize the vulnerability to electromagnetic interferences, all detectors were triaxially cabled and double grounded. A thermal neutron sensor for a Bonner sphere spectrometer should exhibit as high-sensitivity as possible and, at the same time, being photon insensitive and as small as possible. Among the many available thermal neutron sensors [8], ^{3}He is well known to provide the highest sensitivity per unit volume. Of the different commercially available formats, the *VacuTec type 70 060* shows affordable price and well matches the target fixed for the project: accumulating enough counts to produce at least one spectrum per day when the total cosmic neutron fluence rate is about 0.1 cm^{-2} s^{-1}.
- *High-Voltage Supply.* The positive 850 V detector bias is provided by a SILENA 7716/LN generator connected to the 220 V$_{ac}$ line. Said AC line can be very noisy, possibly leading to non-neutron (or false positive) signals to be revealed by the system. To prevent these effects, a 7 μF capacitor filter was interposed between the high-voltage generator and the detectors. A remotely controlled switch allows the high-voltage generator to charge the capacitor for 60 s every 6 h. Consequently, the detectors are permanently isolated from the AC line, except for the very short charging intervals. This cycle was successfully tested up to 8 h between two successive charge intervals.
- *Low-voltage generator.* The analog boards are biased by a $\pm$ 12 V, heavily filtered, low-voltage generator connected to the 220 V$_{ac}$ line.
- *Customized analog boards.* These especially developed multi-input boards include, for every detector, a spectroscopy chain formed by a HV detector bias circuit, a CREMAT CR-110 charge preamplifier and a CREMAT CR-200 shaper amplifier (shaping time 8 μs). All detectors are simultaneously acquired.
- *Digital pulse processing.* The outputs from the analog boards are sent to a 2 MS/s/channel commercial digitizer, model NI 6366, operated by a program written in LabVIEW. The software processes the waveform from the analog boards with the purposes of:
- Discriminating the genuine neutron pulses from photon pulses, relying on a threshold in pulse amplitude (0.3 MeV).
- Discriminating the genuine neutron pulses from the interferences. This is done by comparing the shape of the candidate event with that of the "reference one" in terms of power spectra in the Fourier domain.
  The software also manages the recharge cycles of the high-voltage capacitor filter.
- The stability of the 220 V AC supply is guaranteed by a UPS.

Fig. 2 Geometrical Monte Carlo models used to simulate the response matrix of the 20-cm PE sphere (left) and the 20-cm PE sphere with Fe and Pb metal inserts (right). The numerical values of the response matrix are reported in Fig. 3
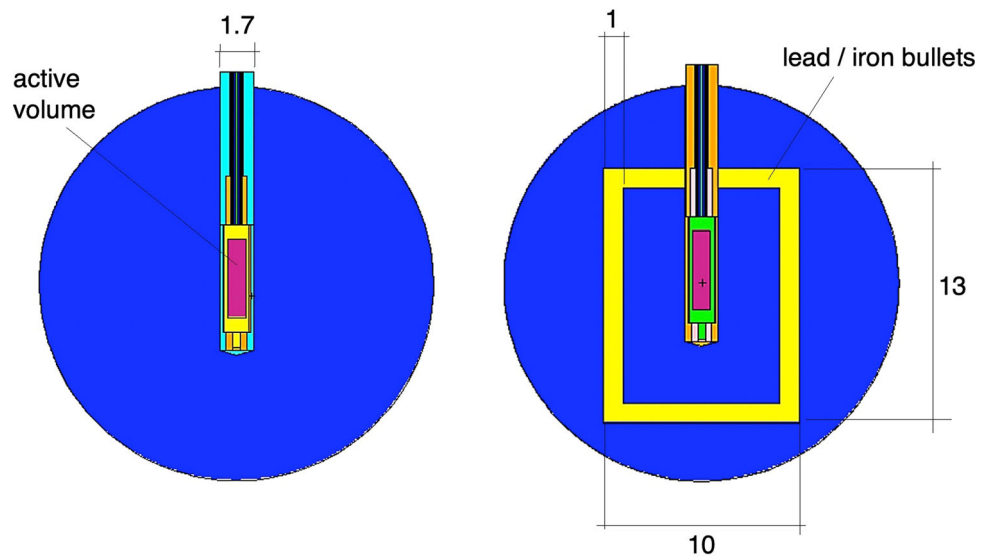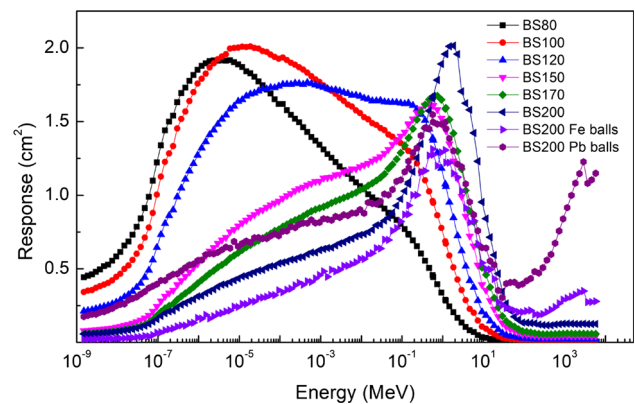

Fig. 3 SAMADHA spheres response matrix calculated using the MCNP code

3 Response matrix

The response functions for the SAMADHA spheres were simulated using the MCNP6 code from 1 meV to 5 GeV. A total of 130 logarithmic equidistant discrete energy bins were chosen for each detector-sphere assembly. The geometrical model (Fig. 2) was built based on the measured dimensions and densities of all materials.

For spheres with Pb- and Fe-balls inserts, their "apparent" density was measured and resulted to be ∼ 60% of the theoretical densities of solid Pb and Fe, respectively. The source, modelled as a disc with the same dimension as the spheres being irradiated, emits parallel neutron beams to the sphere. High-energy interactions were modelled using the Bertini cascade [9, 10] and Dresner evaporation [11–14] models with the RAL fission model [15, 16]. The ENDF/B VIII.0 nuclear data libraries [17] and its thermal neutron scattering $S(\alpha, \beta)$ data were also employed in all the calculations. The h-poly.80t used in the code accounted for thermal neutron scattering by hydrogen bound in polyethylene. The number of counts was assumed to coincide with the number of (n,p) capture reactions in the ^{3}He. According to nominal detector data, the ^{3}He density in the active volume was preliminarily fixed to 1.28×10^{21} ^{3}He atoms cm^{-3}.

The response matrix, calculated with the Monte Carlo code, for all the sphere-detector configuration of the SAMADHA spectrometer is shown in Fig. 3. The matrix is very similar to those of other extended range BSS from the literature [18–21]. The simulated response matrix, $Mi(E)$ (unit: cm^2), is here defined as the number of (n, p) reactions in the ^{3}He counter per unit incident fluence as a function of energy, sphere size, and the monoenergetic neutron energy.

As the number of ^{3}He atoms introduced in the detector model is an a priori estimation, the simulated response of the spectrometer $Mi(E)$ is expected to slightly differ from the experimental response (E). Thus, the purpose of this validation experiment was to determine the scaling factor F_i for each sphere, i.e. the quotient between the experimental and the simulated counts. If the MCNP model is correct and there are no large detector-to-detector differences, F_i should be reasonably constant for all spheres. The degree of constancy of this factor as a function of the sphere diameter is regarded as the "overall accuracy" of the simulated response matrix.
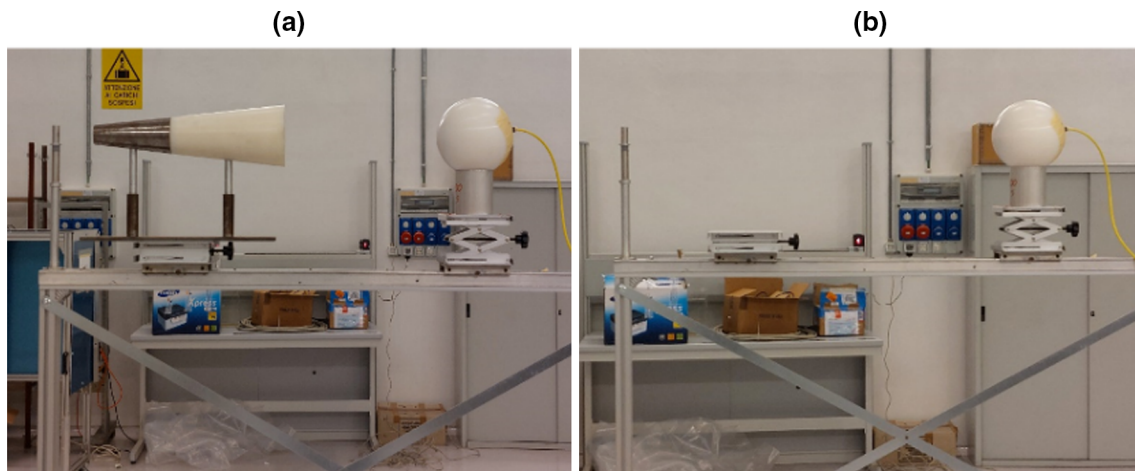
Fig. 4 Experimental calibration set-up (**a**) with and (**b**) without the shadow cone technique

Table 1 Calibration factors

(*) Cones 2, 3, and 4 have a rear Fe diameter of 4.0 cm, and a front PE diameter of 5.5 cm, 6.5 cm, and 9.0 cm, respectively. All cones have a total length of 50 cm

Sphere	SDD (cm)	CONE no. (*)	M_i (Am–Be)	C_i (at SDD = 1 m)	F_i
80	110	2	0.18	1.99 ± 0.06	0.65 ± 0.04
100	100	3	0.40	4.47 ± 0.08	0.65 ± 0.03
120	110	3	0.63	7.25 ± 0.12	0.67 ± 0.03
150	120	3	0.89	10.34 ± 0.15	0.67 ± 0.03
170	140	3	1.03	12.23 ± 0.19	0.69 ± 0.03
200	110	4	1.12	13.07 ± 0.16	0.68 ± 0.03
200 Fe spheres	110	4	0.89	10.46 ± 0.15	0.68 ± 0.03
200 Pb spheres	110	4	1.04	12.43 ± 0.16	0.69 ± 0.03

4 Validation experiment

The SAMADHA Bonner sphere spectrometer was calibrated with the shadow cone technique using a reference ^{241}Am–Be field at the *Politecnico di Milano*. As the spectrum of ^{241}Am–Be slightly varies from source to source according to the capsule size, amount and aggregation properties of the active material, the specific spectrum of this source was previously measured with Bonner spheres [22].

The SAMADHA spectrometer was exposed using the shadow cone technique as recommended in ISO 8529–2 [23]. The shadow cone consists of a 20-cm-long rear iron part and a 30-cm-long front part made of polyethylene. The spheres were placed on an irradiation bench at 190 cm from ground (Fig. 4). The source-to-cone distance was 10 cm. Three shadow cones with different sizes (See Table 1) were available in the facility. According to the sphere diameter, different combinations of cone size and source-to-detector distance (from 110 to 140 cm) were used to maintain the cone shadowing ratio between 1.0 and 2.0 [23]. After subtracting the "cone" measurement from the "total field" measurement, the "net" sphere count rates were corrected to a standard source to detector distance of 100 cm.

The pulse height distributions (PHD) collected by the ^{3}He counters in the different spheres are shown in Figs. 5 and 6. The energy calibration was achieved by attributing the Q-value of the (n,p) reaction (764 keV) to the full-energy peak. The amplitude-to-energy conversion is approximately 1 MeV/V.

From Figs. 5 and 6, as known from basic nuclear measurement literature [24], the rising front at 191 keV corresponds to the complete energy deposited by triton whilst the maximum peak at 764 keV corresponds to the full-energy deposition of both triton and proton. The continuum in the PHD between the peaks is attributed to the "wall effect", i.e. the incomplete absorption of these charged particles when the reaction takes place near the detector walls.

5 Results and discussion

Let:

C_i The "net" (total–cone) count rate in the ith sphere corrected to SDD = 1 m. The experimental counts are derived by integrating the PHD above a fixed conservative threshold of 0.3 MeV to exclude photon-induced signals.

Fig. 5 Pulse height spectra of the SAMADHA spectrometer in semi-log plot for easier discrimination of the spectra for each sphere
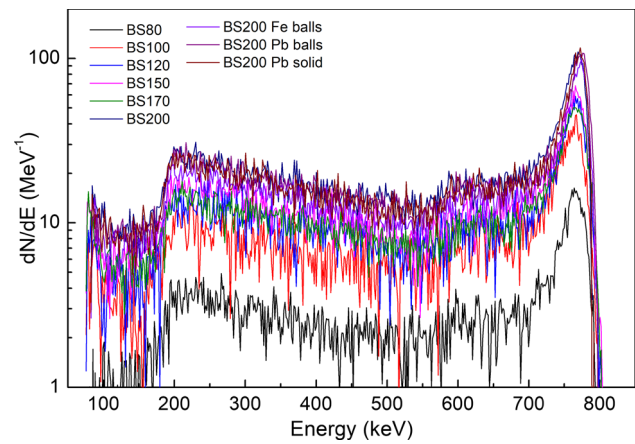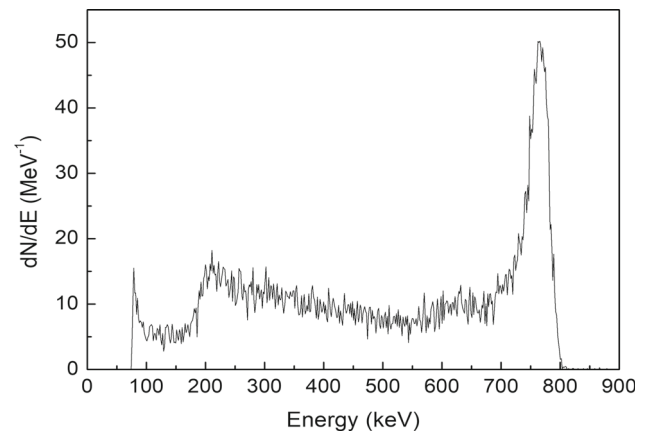

Fig. 6 Pulse height spectrum of the SAMADHA sphere 170 using the ^{3}He proportional counter upon exposure to a ^{241}Am–Be neutron source in linear plot

Φ The un-collided fluence rate at 1 m from the ^{241}Am–Be source $= 17.2 \pm 0.5$ cm^{-2} s^{-1} [22].

$\varphi(E)$ The energy distribution of the ^{241}Am–Be neutron fluence normalized to 1 cm^{-2} or the "unit spectrum" in MeV^{-1}, taken from [22].

$M_i(E)$ The response function of the ith sphere as a function of the energy, in cm^2.

Then the relation between experimental and simulated counts, including the scaling factor F$_i$, is given by:

$$C_i = F_i \Phi \int_{E_{\min}}^{E_{\max}} \varphi(E) M_i(E) \mathrm{d}E \tag{1}$$

where the known computational quantity $\int_{E_{\min}}^{E_{\max}} \varphi(E) M_i(E) \mathrm{d}E$ for the ^{241}Am–Be spectrum is called M$_i$ (^{241}Am–Be).

Using Eq. (1), to derive F_i, the corresponding values are summarized in Table 1. The overall uncertainty of the response matrix, here evaluated as the standard deviation of the F_i values, is as low as 2.3%. It should be noted that, in addition to the differences between the real BSS structure and the simulated model, this uncertainty includes the detector-to-detector variability in terms on number of ^{3}He atoms in the active volume of the detector.

The overall accuracy figure of $\pm 2.3\%$ clearly refers to the energy domain covered by the ^{241}Am–Be source (0.1–12 MeV). Ideally an ERBSS intended for cosmic neutron measurements should be validated in a wider range of reference fields, including high-energy components (E > 20 MeV). Unfortunately, such reference fields are scarcely accessible, being that at iThemba [25] the only one qualified as "reference field". The problem was studied by literature studies including experimental measurements with ERBSS and simulation of their response using different transport codes [26, 27]. As a consolidated conclusion, ERBSS can be used to determine neutron fluence and ambient dose equivalent in cosmic-like neutron fields, with overall accuracy in the order of 10%, provided that their response matrices are:

- Derived with recognized transport codes (such as FLUKA and MCNPX) where adequate intranuclear cascade models are implemented;
- Experimentally validated using commonly available metrology-grade reference fields, such as the ^{241}Am–Be.

Being similar to other established ERBSS, the SAMADHA spectrometer should exhibit enough resolving power to describe the different spectral structures present in environmental neutron spectra. To verify this aspect, a computational exercise was conducted:

Fig. 7 Comparison between the reference, unfolded and guess spectra. All spectra are normalized to the unit fluence and given in lethargic representation
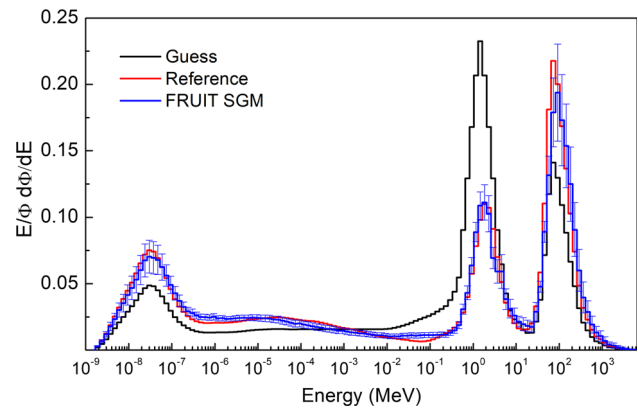
- The spectrum measured with Bonner spheres at the Zugspitze Mountain (elevation 2650 m) was used as a reference spectrum [28].
- This reference spectrum was folded with the calculated SAMADHA response matrix to obtain the expected count rates.
- A 3% perturbation was introduced on the expected count rates.
- The perturbed BSS counts were unfolded using the FRUIT 6 unfolding code in special gradient mode [29, 30].
- To check the resolving power of the response matrix, an intentionally wrong spectrum ("Guess" in Fig. 7) was used as a priori information.

As expected, the resulting unfolded spectrum "FRUIT SGM", shown in Fig. 7, is highly coherent with the reference spectrum. As a standard feature of FRUIT, the bin-per-bin uncertainty superimposed on the unfolded spectrum is derived by propagating input uncertainties (BSS counts and response matrix) through the unfolding process.

If the "FRUIT SGM" spectrum is folded with the response matrix of Fig. 3, multiplied by the scaling factor F (Sect. 5) and the expected total fluence rate that will be found at typical high-elevation sites (at least $0.1\ \mathrm{cm^{-2}\ s^{-1}}$), the expected number of counts well exceeds 10^4/sphere/day, fully matching the SAMADHA target on sensitivity (at least one spectrum per day).

6 Conclusions

An extended range Bonner sphere spectrometer was designed and developed for the SAMADHA project, with special attention to cost, portability, weight, and rejection of spurious signals. Its response matrix, derived with MCNP6, was validated in a reference secondary standard ^{241}Am–Be field at *Politecnico di Milano*, and an overall uncertainty of $\pm 2.3\%$ was estimated. The spectrometer's overall spectrometric performance showed a very good agreement against a typical cosmic neutron spectrum. Further developments will investigate the performance of the spectrometer to high-elevation environment measurements at the CNR Testa Grigia station (3480 m a.s.l. on the Italian-Swiss Alps) in 2022 and, in 2023, measurements in the SAA region.

Data Availability Statement This manuscript has associated data in a data repository. [Authors' comment: The datasets generated during and/or analysed during the current study are available from the corresponding author on reasonable request.]

References

1. F.J. Pavón-Carrasco, A. De Santis, The South Atlantic Anomaly: The key for a possible geomagnetic reversal. Front. Earth Sci. **4**, 40 (2016). https://doi.org/10.3389/feart.2016.00040
2. C.A. Federico et al., Rad. Meas. **45**, 1526 (2010)
3. H. Amit, F. Terra-Nova, M. Lezin, R. Trindade, Non-monotonic growth and motion of the South Atlantic Anomaly. Earths, Planets and Space **73**, 38 (2021). https://doi.org/10.1186/s40623-021-01356-w
4. S.A. Campuzano, M. Gómez-Paccard, F. Pavón-Carrasco, M.L. Osete, Earth Planet. Sci. Lett. **512**, 17 (2019)
5. E.G. Stassinopoulos et al., Forty-Year "Drift" and Change of the SAA. NASA/TM–2015–21754, 2015.
6. ICRP publication 103. The 2007 Recommendations of the International Commission on Radiological Protection. Ann ICRP. 2007;37(2–4):1–332. doi: https://doi.org/10.1016/j.icrp.2007.10.003. PMID: 18082557.
7. R. Bedogni et al., Nucl. Instr. Meth. A **983**, 164595 (2020)
8. A. Pietropaolo, M. Angelone, R. Bedogni, N. Colonna, A.J. Hurd, A. Khaplanov, F. Murtas, M. Pillon, F. Piscitelli, E.M. Schooneveld, K. Zeitelhack, Phys. Rep. **875**, 1 (2020)
9. H.W. Bertini, Bertini. Phys. Rev. **131**, 1801 (1963)
10. H.W. Bertini, Bertini. Phys. Rev. **188**, 1711 (1969)
11. L. Dresner, EVAP – A Fortran Program for Calculation the Evaporation of Various Particles from Excited Compound Nuclei, Oak Ridge National Laboratory Report ORNL-TM196, 1962

12. M. P. Guthrie EVAP-2 and EVAP-3: Modifications of a Code to Calculate Particle Evaporation from Excited Compound Nuclei, Oak Ridge National Laboratory Report ORNL-4379, 1969 March, 36 pp
13. M. P. Guthrie, EVAP-4: Another Modification of a Code to Calculate Particle Evaporation from Excited Compound Nuclei, Oak Ridge National Laboratory Report ORNL-TM-3119, 1970
14. P. Cloth, D. Filges, G. Sterzenbach, T. W. Armstrong, B.L. Colborn, The KFA-Version of the High-Energy Transport Code HETC and the Generalized Evaluation Code SIMPEL, Kernforschungsanlage J¨ulich Report J¨ul-Spez-196, 1983.
15. RAL F. Atchison, Spallation and Fission in Heavy Metal Nuclei under Medium Energy Proton Bombardment, in Proc. Meeting on Targets for Neutron Beam Spallation Source, Julich, June 11–12, 1979, pp. 17–46, G. S. Bauer, Ed., Jul-Conf-34, Kernforschungsanlage Julich GmbH, Germany (1980)
16. A Treatment of Fission for HETC, in Intermediate Energy Nuclear Data: Models and Codes, pp. 199–218 in Proceedings of a Specialists's Meeting, May 30–June 1, 1994, Issy-Les-Moulineaux, France, OECD, Paris, France (1994).
17. D.A. Brown et al., ENDF/B-VIII.0: The 8th major release of the nuclear reaction data library with CIELO-project Cross sections, new standards and thermal scattering data. Nucl. Data Sheets **148**, 1–142 (2018)
18. R. Bedogni et al., Rad. Meas. **45**, 1201 (2010)
19. V. Vylet, Nucl. Instr. Meth. A **476**, 26 (2002)
20. R. Bedogni, Rad. Prot. Dosim. **146**, 383 (2011)
21. R. García-Baonza, G.F. García-Fernández, L.E. Cevallos-Robalino, E. Gallego, Appl. Rad. Isot. **163**, 109196 (2020)
22. A. Pola et al., Nucl. Instr. Methods A **927**, 371 (2019)
23. ISO 8529–2, Reference neutron radiations — Part 2: Calibration fundamentals of radiation protection devices related to the basic quantities characterizing the radiation field. 17.240 Radiation measurements, 2000.
24. G.F. Knoll, *Radiation Detection and Measurement*, 4th edn. (Wiley, New York, 2010)
25. A. Buffler, G. Reitz, S. Röttger, F. D. Smit, F. Wissmann (Eds.). Irradiations at the High-Energy Neutron Facility at iThemba LABS. EURADOS Report 2016–02. 2016.
26. C. Pioch, V. Mares, W. Rühm, Rad. Meas. **45**, 263 (2010)
27. S. Agosteo, R. Bedogni, M. Caresana, N. Charitonidis, M. Chiti, A. Esposito, M. Ferrarini, C. Severino, M. Silari, Nucl. Instr. Meth. A. **694**, 55 (2012)
28. S. Barros, V. Mares, R. Bedogni, M. Reginatto, A. Esposito, I. Gonçalves, P. Vaz, W. Rühm, Comparison of unfolding codes for neutron spectrometry with Bonner spheres. Radiat. Prot. Dosimetry **161**, 46 (2014)
29. R. Bedogni, C. Domingo, A. Esposito, F. Fernandez, Nucl. Instr. Meth. A **580**, 1301 (2007)
30. K. Amgarou, R. Bedogni, C. Domingo, A. Esposito, A. Gentile, G. Carinci, S. Russo, Nucl. Inst. Meth. A **654**, 399 (2011)